AIAA JOURNAL
Vol. 38, No. 9, September 2000

Effects of Structural Damping and Stiffness on Impact Response of Layered Structure

S. W. Gong* and K. Y. Lam†
Institute of High Performance Computing, 118261 Singapore, Republic of Singapore

The transient response of layered structures subjected to low-velocity impact is dealt with. A spring–mass model is improved by implementing the structural damping to determine the contact force between the target and striker during impact. Based on this model, an analytic function describing the contact force is derived in terms of the material properties, structural mass, impact mass, and velocity, as well as the structural damping. A finite element approach (FEA) is proposed for the prediction of transient response of layered structures subjected to low-velocity impact. In the FEA, the present impact force function is linked into a commercial code in which the effects of effective structural damping and stiffness are incorporated. The present impact force function is verified by the experiment, and the FEA is verified by comparing the present results with previously published results. In addition, effects of structural damping and stiffness on transient response of layered structure subjected to low-velocity impact are examined in detail.

I. Introduction

IMPACT on composite structures has been a subject of considerable interest and concern in recent years. Sun and Chattopadhyay[1] and Dobyns[2] used the plate equations developed by Whitney and Pagano[3] to analyze a simply supported, special orthotropic plate subjected to central impact. Ramkumar and Thakar,[4] using Donnell's equations for thin shells, presented an analysis of the response of curved laminated plates under low-velocity impact. They assumed that the impact force varies linearly with time and adopted the Dobyns[2] solution procedure.

Christoforou and Swanson[5] formulated an analytic solution to the problem of simply supported, orthotropic cylindrical shells subjected to impact loading. In their analysis, the deceleration of the impacting mass was used to estimate the impact force. Gong et al.[6–8] and Shim et al.[9] adopted Christoforou and Swanson's[5] approach and undertook an analysis of laminated, open cylindrical shells subjected to impact. In Refs. 6–9, contact deformation was considered, and an analytic function describing it was proposed and incorporated into the analysis. The solution facilitates study of transient response of composite shells impacted by a solid striker at any arbitrary location.

Lu and Lam[10] presented a numerical method for fully clamped laminated composite plates subjected to low-velocity impact of a mass. Hertzian contact law was also used to describe the contact force whereas the Runge–Kutta–Nytron technique was used to solve the governing equation. Recently, Gong et al.[11] presented solutions for the problems of functionally graded material cylindrical shells subjected to low-velocity impact.

As noted, much effort has been made to analyze composite plates and shells subjected to low-velocity impact. However, none of those studies considered the effects of structural damping on the transient response, and thus an analysis procedure that includes the structural damping has not yet been dealt with. Because structural damping can be used to attenuate transient response of the target to impact, a comprehensive study of structural damping effects is necessary for the optimal design of layered structures. The present work addresses this, and presents a finite element approach (FEA) for the problem involving effective structural damping and stiffness.

In this study, the analytic function proposed by Gong et al.,[6] describing the contact force is improved upon in terms of the material properties, structural mass, impact mass, and velocity, as well as the structural damping. The present impact force function is linked into a commercial code in which the effects of effective structural damping and stiffness are incorporated. Information on the effects of effective damping and stiffness on the impact response is useful in designing layered structures to enhance their resistance to impact.

II. Analysis Procedure

Consider a two-layered composite panel as shown in Fig. 1. It is impacted at an arbitrary location by a solid striker at a velocity V. The two-layer composite panel consists of a basic elastic layer and a damping layer. The basic elastic layer has a thickness of h_1, Young's modulus E_1, and loss factor η_1, and the damping layer has a thickness of h_2, Young's modulus E_2, and loss factor η_2. The panel has a common length of L and width of W for both the basic elastic and the damping layers.

In this study, a simple spring–mass–damping (S–M–D) model is proposed. It is essentially a modification of the spring–mass (S–M) model (Fig. 2a), implementing the effective structural damping, and is shown in Fig. 2b.

In reality, the impact force is a result of contact deformation between the striker and the target structure and should, thus, be evaluated on this basis. Let $w(t)$ and $w_2(t)$ represent, respectively, the normal displacement of the load point on the panel and that of the striker at any time t during impact. C_e and η_{st} are the effective damping coefficient and the effective structural loss factor of the two-layered composite panel, respectively, and they are related by

$$C_e = \eta_{st} K_1 / \omega_{11} \tag{1}$$

where K_1 is the equivalent stiffness of the panel and ω_{11} is the fundamental frequency of the layered panel. The equations of motion of the two-degree-of-freedom S–M system are, therefore,

$$m_{1e}\ddot{w} + C_e\dot{w} + (K_1 + K_2)w - K_2 w_2 = 0 \tag{2a}$$

$$m_2\ddot{w}_2 - K_2 w + K_2 w_2 = 0 \tag{2b}$$

in which K_2 is the effective contact stiffness, which can be determined by an impact test or estimated by[6]

$$K_2 = \sqrt{\pi}\,\Gamma\left(\frac{p+1}{2}\right)\frac{2\Gamma(p/2+1) + \sqrt{\pi}\,\Gamma[(p+1)/2]}{4\Gamma^2(p/2+1) + \pi\Gamma^2[(p+1)/2]}\,\delta_m^{p-1}K_c \tag{3}$$

where $\Gamma(x)$ is the gamma function, the contact coefficients K_c and p are defined by Hertzian theory of the form $F(t) = K_c[\delta(t)]^p$, and

Received 22 March 1999; revision received 16 September 1999; accepted for publication 27 December 1999.

*Principal Research Engineer, 89C Science Park Drive, No. 02-11/12, The Rutherford, Singapore Science Park 1.

†CEO and Director, 89C Science Park Drive, No. 02-11/12, The Rutherford, Singapore Science Park 1.

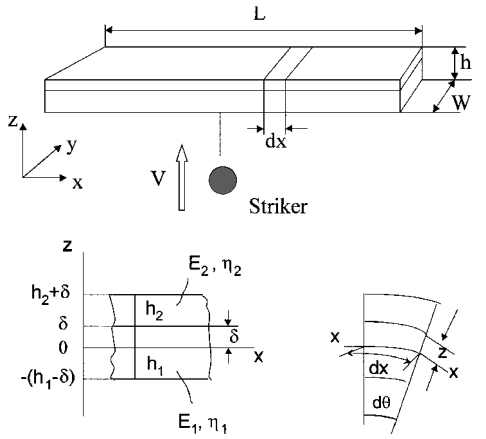

Fig. 1 Description of the problem, layered beam geometry, and coordinator system.

δ_m is the maximum contact deformation. For a striker of small mass ($m_{1e} > 10_{m2,}$), δ_m can be estimated by

$$\delta_m = \left(\frac{m_{1e}m_2}{m_{1e}+m_2}\right)^{1/(p+1)}\left(\frac{p+1}{2}\right)^{1/(p+1)}\left(\frac{V^2}{K_2}\right)^{1/(p+1)} \tag{4}$$

where m_{1e} is the effective target mass determined from

$$m_{1e} = \rho h \int_{A_p}\int W^2(x, y)\,\mathrm{d}A_p$$

in which $\mathrm{d}A_p$ is the differential surface area of the target structure, A_p is the total area, $W(x, y)$ is a function of position that defines the shape of the natural mode of the target structure vibration, and m_2 is the impact mass of the striker. Note that the geometry of the target structure in the S–M–D model is not restricted; it can be shell or plate.

The contact force is expressed in the form

$$F(t) = K_2[w_2(t) - w(t)] \tag{5}$$

Equations (2a) and (2b) are solved, and the solutions to $w(t)$ and $w_2(t)$ are substituted into Eq. (5) with the initial conditions

$$w = \dot{w} = w_2 = 0, \qquad \dot{w}_2 = V \quad \text{at} \quad t = 0 \tag{6}$$

This yields an analytic function for the estimation of contact force during impact:

$$F(t) = \begin{cases} K_2[a_1(c_1-1)\sin(\omega_{1e}t) + a_2(c_2-1)\sin(\omega_2 t)] & 0 < t < T \\ 0 & t > T \end{cases} \tag{7}$$

where

$$\omega^2_{1e,2} = \frac{1}{2}\left[\frac{K_1+K_2}{m_{1e}(1-\eta_{\mathrm{st}})} + \frac{K_2}{m_2}\right] \mp \sqrt{\frac{1}{4}\left[\frac{K_1+K_2}{m_{1e}(1-\eta_{\mathrm{st}})} - \frac{K_2}{m_2}\right]^2 + \frac{K_2^2}{m_{1e}m_2(1-\eta_{\mathrm{st}})}}$$

$$c_1 = \frac{K_2}{K_2 - \omega_{11}^2 m_2}, \qquad c_2 = \frac{K_2}{K_2 - \omega_2^2 m_2}$$

$$a_1 = \frac{V}{\omega_{11}(c_2 - c_1)}, \qquad a_2 = \frac{V}{\omega_2(c_1 - c_2)} \tag{8}$$

The present force function is implemented in the commercial software LS-DYNA3D.[12] The impact force was first predicted by a FORTRAN program based on the force function (1), the output of which is formatted in key words readable by LS-DYNA3D. The force function is expressed in terms of the material properties, stiffness and mass of both the striker and the target structure, and the initial velocity of the striker, as well as the structural damping. Thus, it is appropriate for the description of the layered panel impacted by a solid striker at a low velocity and for the determination of the contact force between the striker and the layered panel. In this way, the commercial software is employed only for modeling the layered panel (without the striker), whereas the presented force function is implemented to handle the contact force between the striker and the layered panel. Therefore, the problem of impact on the layered composite structure is simplified to solve a standard structural response equation of motion for a known impact (dynamic) loading:

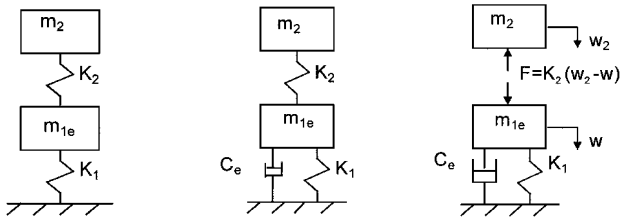

Fig. 2 Models.

$$[M_s]\{\ddot{\chi}\} + [C_s]\{\dot{\chi}\} + [K_s]\{\chi\} = \{f\} \tag{9}$$

where $\{\chi\}$ is the element displacement vector; $[M_s]$, $[C_s]$, and $[K_s]$ are the structural mass, damping, and stiffness matrices; $\{f\}$ is the dynamic loading vector that can be determined from Eq. (7); and a dot denotes a temporal derivative. Equation (9) can be readily solved with any numerical integration procedure. This provides a connection between the Hertz contact force law for layered structures with a well-established finite element software, and, thus, more realistic and complex structure subjected to impact can be simulated easily without the restriction to the boundary conditions.

III. Effective Structural Damping and Stiffness

The effective structural loss factor η_{st} is derived using the complex stiffness method that was proposed by Oberst[13]; the effective Young's modulus E_{st} is derived using the minimum potential energy principle.

A. Effective Structural Loss Factor for the Two-Layer Composite Beam

The energy dissipating effects of the material damping are considered, and, thus, Young's moduli for the basic layer and the damping layer are complex quantities that are denoted by a superscript asterisk. The strain of the beam is

$$\varepsilon = \frac{z\,\mathrm{d}\theta}{\mathrm{d}x} = \frac{z}{j\omega_{11}}\frac{\partial}{\partial x}\left(\frac{\partial\theta}{\partial t}\right) \tag{10}$$

The axis stress of the beam is expressed as

$$\sigma_i = E_i^*\varepsilon = \frac{E_i^*}{j\omega_{11}} z\frac{\partial}{\partial x}\left(\frac{\partial\theta}{\partial t}\right) \qquad (i = 1, 2) \tag{11}$$

For pure bending of the beam,

$$\int_{-(h_1-\delta)}^{h_2+\delta} \sigma_i\,\mathrm{d}z = \frac{1}{j\omega_{11}}\frac{\partial w}{\partial x}\int_{-(h_1-\delta)}^{h_2+\delta} E_i^* z\,\mathrm{d}z = 0 \tag{12}$$

Note that $(1/j\omega_{11})(\partial/\partial x)(\partial\theta/\partial t) \neq 0$. From the equation

$$\int_{-(h_1-\delta)}^{\delta} E_1^* z\,\mathrm{d}z + \int_{\delta}^{h_2+\delta} E_2^* z\,\mathrm{d}z = \frac{1}{2}E_2^* h_2^2 + E_2^* h_2\delta$$

$$-\frac{1}{2}E_1^* h_1^2 + E_1^* h_1\delta = 0 \tag{13}$$

the neutral axis position can be obtained:

$$\delta = \frac{1}{2}\frac{E_1^* h_1^2 - E_2^* h_2^2}{E_1^* h_1 + E_2^* h_2} \tag{14}$$

Because the loss factor in the basic elastic layer is much lower than that in the damping layer, that is, $\eta_1 \ll \eta_2$, the effect of η_1 can be ignored, and, thus, Eq. (14) becomes

$$\delta = \frac{1}{2}\frac{h_1 - h_2\lambda_e^*\lambda_h}{\left(1 + \lambda_e^*\lambda_h\right)} \tag{15}$$

where

$$\lambda_e^* = E_2^*\big/E_1 = (E_2/E_1)(1 + j\eta_2) = \lambda_e(1 + j\eta_2) \tag{16}$$

and $\lambda_h = h_2/h_1$ and $\lambda_e = E_2/E_1$.

The complex bending stiffness can be calculated by

$$B^* = \int_{-(h_1-\delta)}^{\delta} E_1 z^2\,\mathrm{d}z + \int_{\delta}^{h_2+\delta} E_2^* z^2\,\mathrm{d}z$$

$$= B_1\frac{1 + 2\lambda_e^*\left(2\lambda_h + 3\lambda_h^2 + 2\lambda_h^3\right) + \lambda_e^{*2}\lambda_h^4}{\left(1 + \lambda_e^*\lambda_h\right)} \tag{17}$$

where $B_1 = E_1 I_1$. The effective loss factor and the complex bending stiffness is related by

$$B^* = B_{\mathrm{st}}(1 + j\eta_{\mathrm{st}}) \tag{18}$$

Substituting Eq. (16), in conjunction with Eq. (18), into Eq. (17) yields

$$\frac{B_{\mathrm{st}}(1 + j\eta_{\mathrm{st}})}{B_1} = \frac{1 + 2\lambda_e(1 + j\eta_2)\left(2\lambda_h + 3\lambda_h^2 + 2\lambda_h^3\right) + \lambda_e^2(1 + j\eta_2)^2\lambda_h^4}{1 + \lambda_e\lambda_h(1 + j\eta_2)} \tag{19}$$

Taking both sides of Eq. (19) to be equal in imaginary component yields

$$\frac{\eta_{\mathrm{st}}}{\eta_2} = \frac{\lambda_e\lambda_h}{(1 + \lambda_e\lambda_h)} \times \frac{3 + 6\lambda_h + 4\lambda_h^2 + 2\lambda_e\lambda_h^3 + \lambda_e^2\lambda_h^4}{1 + 2\lambda_e\left(2\lambda_h + 3\lambda_h^2 + 2\lambda_h^3\right) + \lambda_e^2\lambda_h^4} \tag{20}$$

Equation (20) shows that the effective structural loss factor η_{st} can be obtained from the loss factor of the damping layer if Young's modulus ratio and the thickness ratio of the damping and the basic layers are known.

B. Effective Young's Modulus for the Two-Layer Composite Beam

Consider the differential elements of the two-layer beam subjected to constant unidirectional strain $\varepsilon_x = \varepsilon$; the potential energy per unit is

$$U = \tfrac{1}{2}E_{\mathrm{st}}\varepsilon^2 \tag{21}$$

Assume

$$\varepsilon_y = \varepsilon_z = \nu_{\mathrm{st}}\varepsilon \tag{22}$$

The relation of strain and stress is expressed by

$$\sigma_x = [\lambda(1 + 2\nu_{\mathrm{st}}) + 2G]\varepsilon \tag{23}$$

$$\sigma_y = \sigma_z = [\lambda(1 + 2\nu_{\mathrm{st}}) + 2G\nu_{\mathrm{st}}]\varepsilon \tag{24}$$

where

$$\lambda = \frac{E_{\mathrm{st}}\nu_{\mathrm{st}}}{(1 + \nu_{\mathrm{st}})(1 - 2\nu_{\mathrm{st}})}, \qquad G = \frac{E_{\mathrm{st}}}{2(1 + \nu_{\mathrm{st}})}$$

Let ν_1 and ν_2 denote Poisson's ratios of the damping layer and the basic elastic layer, respectively. For the possible displacement state, the strain energy density is

$$U^{(s)} = \frac{1}{2}(\sigma_{1x}\varepsilon_x + \sigma_{1y}\varepsilon_2 + \sigma_{1z}\varepsilon_3)\frac{h_1}{h} + \frac{1}{2}(\sigma_{2x}\varepsilon_x + \sigma_{2y}\varepsilon_2 + \sigma_{2z}\varepsilon_3)\frac{h_2}{h}\frac{1}{2}\varepsilon^2\left[\frac{1 - \nu_1 + 4\nu_1\nu_{\mathrm{st}} + 2\nu_{\mathrm{st}}^2}{1 - \nu_1 - 2\nu_1^2}E_1\frac{h_1}{h} + \frac{1 - \nu_2 + 4\nu_2\nu_{\mathrm{st}} + 2\nu_{\mathrm{st}}^2}{1 - \nu_2 - 2\nu_2^2}E_2\frac{h_2}{h}\right] \tag{25}$$

From $\partial U^{(s)}/\partial\nu_{\mathrm{st}} = 0$ and $\partial^2 U^{(s)}/\partial\nu^2 > 0$, the coefficient ν_{st} can be selected by

$$\nu_{\mathrm{st}} = \frac{\left(1 - \nu_1 - 2\nu_1^2\right)\nu_2\lambda_e\lambda_h + \left(1 - \nu_2 - 2\nu_2^2\right)\nu_1}{\left(1 - \nu_1 - 2\nu_1^2\right)\lambda_e\lambda_h + \left(1 - \nu_2 - 2\nu_2^2\right)} \tag{26}$$

From the minimum potential energy principle $U^{(s)} \geq U$, the effective Young's modulus can be obtained:

$$E_{\mathrm{st}} = \left(\frac{1 - \nu_1 + 4\nu_1\nu_{\mathrm{st}} + 2\nu_{\mathrm{st}}^2}{1 - \nu_1 - 2\nu_1^2} + \frac{1 - \nu_2 + 4\nu_2\nu_{\mathrm{st}} + 2\nu_{\mathrm{st}}^2}{1 - \nu_2 - 2\nu_2^2}\lambda_e\lambda_h\right)E_1\frac{h_1}{h} \tag{27}$$

For the case of $\nu_1 = \nu_2 = \nu_{\mathrm{st}}$, Eq. (19) can be simplified as

$$E_{\mathrm{st}} = (1 + \lambda_e\lambda_h)E_1(h_1/h) \tag{28}$$

Equations (20) and (27) can be used to determine the effective structural damping and stiffness of the layered beam, the outcome of which can then be incorporated into the structural damping and stiffness matrices in Eq. (9). This facilitates a study of structural damping and stiffness effects on transient response of the layered beam subjected to impact.

IV. Correlation Studies

The validity of the present approach is established by comparing its predictions with published results that were validated by impact experiments. First, the contact force was measured and calculated for the case that a 0.075-kg impact mass at a velocity of 1 m/s strikes a $[0_8]$ glass/epoxy cylindrical shell. The shell has a mean radius of 0.108 m, a length of 0.28 m, and a thickness of 2.3 mm, and the material properties are $E_{11} = 14.51$ GPa, $E_{22} = 5.36$ GPa, $G_{12} = 2.51$ GPa, $\nu_{12} = 0.231$, and $\rho = 1901.5$ kg/m^3. These geometry and material data are taken from Ref. 8, in which the measurement of the contact force was presented in detail.

Figure 3 shows the contact forces obtained from the impact experiment,[8] the previous force function (S–M model),[8] and the present force function (S–M–D model), respectively. It is observed that the force–time curves obtained from present and previous impact force function are almost the same, with the present peak force being slightly less than that calculated by the previous one. This illustrates that the structural damping has only a slightly effect on contact force, which makes the present contact force slightly closer to the experiment contact force. A comparison between the present

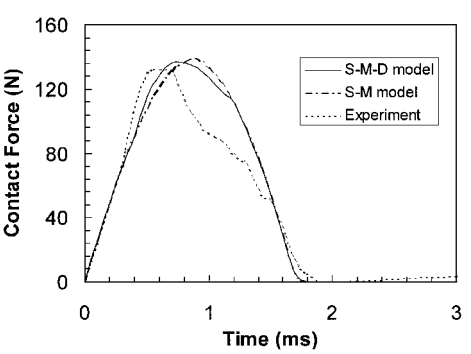

Fig. 3 Contact force vs time for a $[0_8]$ glass/epoxy cylindrical shell impacted by a 0.075 mass at a velocity of 1 m/s.

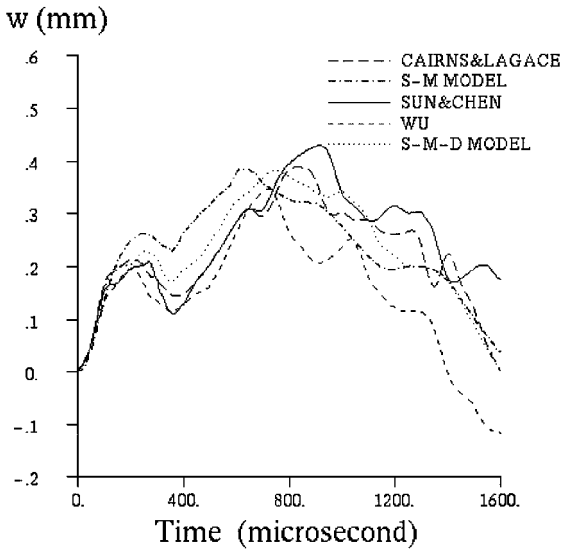

Fig. 4 Center displacement vs time for a T300/934 graphite/epoxy plate impacted by a 12.7-mm-diam steel ball at 3 m/s velocity.

values and the experiment results show that the present contact duration and peak force differ from the measured values by at most 5%. Also the present force–time curve matches the measured one reasonably well.

The other case is a 200 × 200 mm T300/934 graphite/epoxy plate in a $[90/0/90/0/90]_s$ configuration. The plate is simply supported and impacted by a 12.7-mm-diam steel ball at a velocity of 3 m/s. This case is calculated because results for this particular configuration have been verified experimentally by Sun and Chen[14] with good correlation. The constitutive properties utilized for the basic T300/934 ply are $E_{11} = 141.2$ GPa, $E_{22} = 9.72$ GPa, $\nu_{12} = 0.3$, $\nu_{23} = 0.3$, $G_{12} = 5.53$ GPa, and $G_{23} = 3.74$ GPa, with a mass density of 1536 kg/m^3 and a per ply thickness of 0.269 mm.

Figure 4 shows displacement vs time of impact for the simply supported $[0/90/0/90/0]_s$ T300/934 graphite/epoxy plate. Sun and Chen[14] and Wu[15] used finite element methods to obtain their solutions whereas Cairns and Lagace[16] used a Rayleigh–Ritz energy method in their study. The results obtained by the present approach are compared with Refs. 14–16. It is observed that the displacement curve of the S–M model exhibits a higher value for the first peak, and then reaches its second peak value earlier than results reported by the other authors. This may be expected because a linearization of the Hertzian contact force-deformation relationship was assumed in the S–M model, which causes a slightly higher prediction of the impact force during the contact duration[6] and, thus, effects the results of the S–M model.

The comparison of the curves between the S–M–D model and the S–M model shows that the first peak of the present S–M–D model is reduced by 6%, and also a slower rising time for the second peak of the present S–M–D model is observed. This is due to the damping effects that are included in the S–M–D model so that an improvement on the prediction of the contact force and the resulting displacement is obtained. Figure 4 also indicates that the present S–M–D model give a more reasonable match with those published by Refs. 14–16.

V. Effects of Structural Damping and Stiffness

Effects of structural damping and stiffness on the transient response of a layered beam to impact were investigated. The layered beam has a length of 1 m, a width of 0.1 m, and a total thickness of 0.04 m. The material properties of the basic layer are $E_1 = 210$ GPa, $\nu_1 = 0.3$, and $\rho_1 = 7850$ kg/m^3. Poisson's ratio and the density the damping layer is assumed to be 0.4 and 980 kg/m^3 whereas the Young's modulus of the damping layer varies with the modulus ratio $\lambda_e = E_2/E_1$. In this study, the thickness of the beam is kept constant while the thickness of the damping layer and the basic elastic layer vary with the thickness ratio $\lambda_h = h_2/h_1$. The effective Young's modulus and Poisson's ratio for the layered beam are calculated using Eqs. (26) and (27). The effective density for the layered beam is evaluated by $\rho_{st} = (1 + \lambda_\rho \lambda_h)(h_1/h)\rho_1$ and $\lambda_\rho = \rho_2/\rho_1$.

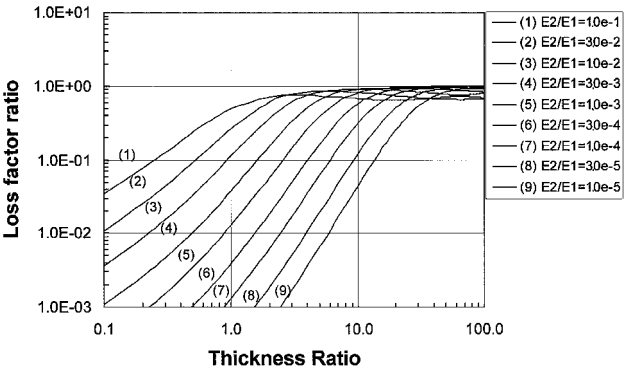

Fig. 5 Variations of loss factor ratio η_{st}/η_1 with thickness ratio $\lambda_h = h_2/h_1$.

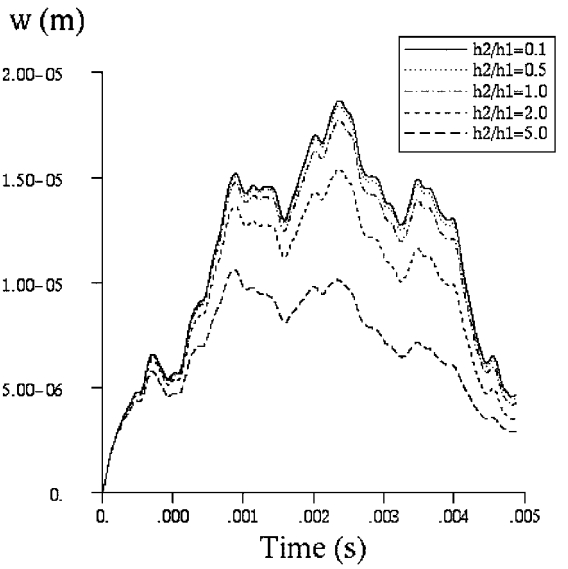

Fig. 6 Central displacement vs time for different thickness ratios.

Figure 5 shows the variations of the loss factor ratio η_{st}/η_2 with the thickness ratio λ_h. The loss factor ratio is proportional to the thickness ratio λ_h and the modulus ratio λ_e for small thickness ratio, whereas it approaches unity for a very large thickness ratio. This corresponds to Eq. (20) in which the loss factor ratio approaches $3\lambda_e\lambda_h$ as λ_h tends to zero, whereas the loss factor ratio approaches unity as λ_h tends to be infinite. Inspection of Fig. 5 shows that for a smaller modulus ratio, increasing the thickness of damping layer has no effect on the shock attenuation of the layered beam. For example, when $\lambda_e = E_2/E_1 \leq 1.0e{-}5$, even though the thickness of the damping layer is increased to three times of the thickness of the basic elastic layer, that is, $\lambda_h = 3$, the effective loss factor for the layered beam λ_{st} is only 1000th as much as the loss factor of the damping layer λ_2. It follows that only for the larger modulus ratio λ_e the loss factor ratio increases with the thickness ratio. In other words, only for a larger modulus ratio can the damping effects be enhanced by increasing the thickness of the damping layer. To affect the shock attenuation, the optimal damping material should have lightweight, high modulus and high loss factor.

Figure 6 shows central displacement-time histories for different thickness ratios. In this study, the modulus ratio is assumed to be $\lambda_e = E_2/E_1 = 1.0e{-}1$. It is observed that for a small thickness ratio ($\lambda_h \leq 0.5$), the displacement decreases slightly with the thickness ratio, with only 2% difference in their peak displacement values at most. As the thickness ratio increases from $\lambda_h = 0.5$, the displacement begins to reduce rapidly with the thickness ratio. The peak displacement value for $\lambda_h = 2$ is reduced by 20%, and the peak displacement value for $\lambda_h = 5$ is further reduced by 85%. This result

shows that, for $\lambda_e = 1.0e-1$, the structural damping of the layered beam becomes effective as λ_h becomes larger than 0.5.

Figure 7 shows central displacement-time histories for different modulus ratios. In this study, the thickness ratio is assumed to be $\lambda_h = 1.0$. It is observed that the peak value and duration of the central displacement decrease with the modulus ratio increasing. This is expected because the effective modulus of the layered beam increases as the modulus ratio increases, which in turn increases the value of the fundamental frequency of the beam and, thus, reduces the peak value and duration of the central displacement. The results in Figs. 6 and 7 illustrate both thickness and modulus ratios have significant effects on the impact response.

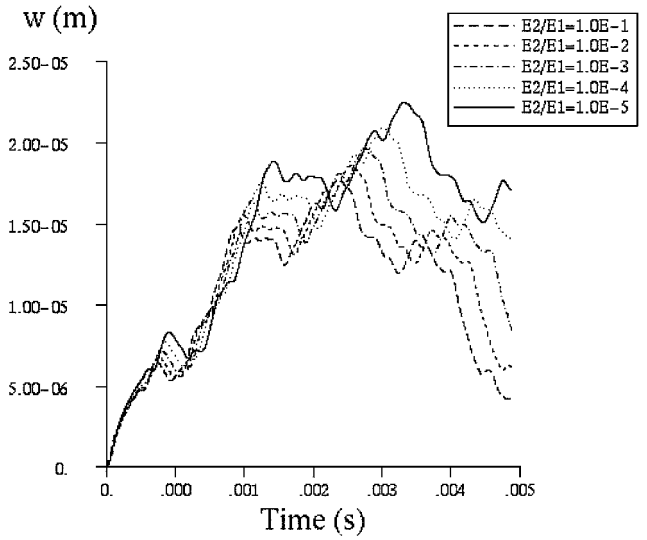

Fig. 7 Central displacement vs time for different modulus ratios.

Figure 8 shows fringe levels for the transverse displacement of the layered beam for different thickness ratios, at the instant of $t = 2.866$ ms, when the central displacements reach their peak values. It is observed that the flexural wave moves toward the beam ends slower for the larger thickness ratio, which corresponds to a higher effective damping factor. As we know, the frequency decreases as the effective structural loss factor increases and, therefore, it decreases as the thickness ratio increases. (Note that both the phase and group speed for the flexural wave in the layered beam is proportional to the square root of the frequency and to the fourth root of E_{st}/ρ_{st}.) This is one reason the speeds of the flexural wave reduce as the thickness ratio increases.

On the other hand, the fourth root of E_{st}/ρ_{st} can be expressed as

$$\left(\frac{E_{st}}{\rho_{st}}\right)^{\frac{1}{4}} = \left(\frac{E_1}{\rho_1}\right)^{\frac{1}{4}} \left[\frac{(1+\lambda_e\lambda_h)}{(1+\lambda_\rho\lambda_h)}\right]^{\frac{1}{4}} \tag{29}$$

In this study, $\lambda_e = 3.0e-3$ and $\lambda_\rho = 1.26e-1$. As λ_h approaches zero, $(E_{st}/\rho_{st}) \approx (E_1/\rho_1)$, the effects of the density ratio can be ignored. For $\lambda_h > 1$, the fourth root of E_{st}/ρ_{st} may decreases with the thickness ratio λ_h because the density ratio is much larger than Young's modulus ratio. This explains why the speeds of the flexural wave reduce more for a larger value of the thickness ratio. This also indicates that the structural damping has a significant effect on the flexural wave propagation.

The variation of the relative effective modulus E_{st}/E_2 for the two-layer composite beam with the material and geometry parameters λ_h and λ_e is plotted in Fig. 9. In this study, the modulus ratio ranges from $1.0e-5$ to $1.0e-1$. For a smaller thickness ratio, $\lambda_h \leq 1.0$, the relative effective modulus decrease slowly as the thickness ratio increases; however, for a large thickness ratio, $\lambda_h \geq 10$, the relative effective modulus decreases much more rapidly for the large modulus ratio. At thickness ratio $\lambda_h = 10$, the relative effective modulus for $\lambda_e = 1.0e-1$ is about twice as much as that for $\lambda_e = 1.0e-5$.

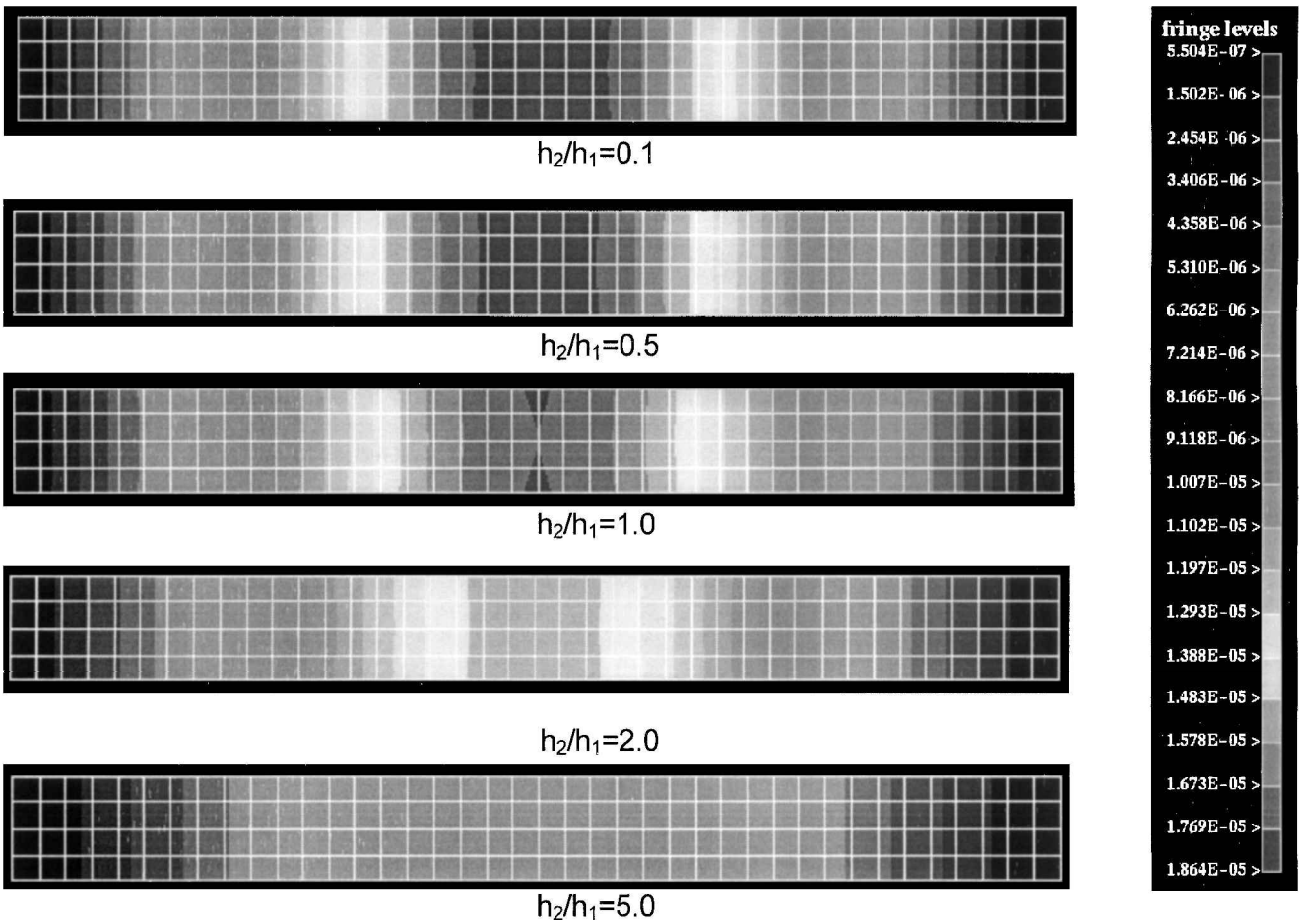

Fig. 8 Fringe levels for the transverse displacement of the layered beam for different thickness ratios at $t = 2.866$ ms.

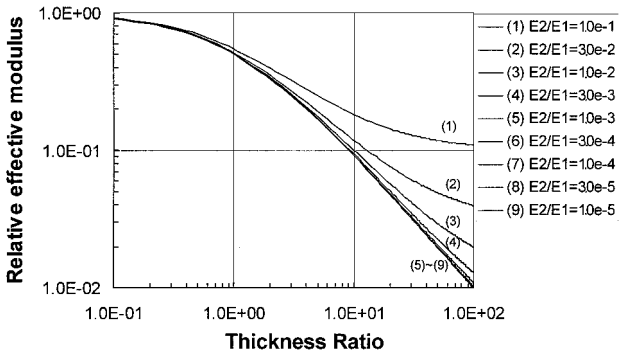

Fig. 9 Variation of relative effective modulus E_{st}/E_2 with thickness ratio $\lambda_h = h_2/h_1$.

Furthermore, at the thickness ratio $\lambda_h = 100$, the relative effective modulus for $\lambda_e = 1.0e-1$ is about 11 times as much as that for $\lambda_e = 1.0e-5$. This result suggests that the smaller thickness ratio should be used in the structural design of the two-layer composite beam, and, thus, the stiffness of the composite beam may be close to that of the basic elastic layer.

VI. Conclusions

An FEA was proposed for prediction of transient response of layered structures subjected to low-velocity impact. In the present approach, the improved impact force function is linked to a commercial code in which the effects of effective structural damping and stiffness are incorporated. The present approach facilitates investigation of the effects of structural damping and stiffness on the transient response of layered structures subjected to low-velocity impact. The results show that both thickness and modulus ratios have significant effects on the impact response. The results also show that the structural damping greatly influences the flexural wave propagation. In addition, the results suggest that to affect the shock attenuation, the optimal damping material should have a light weight, a high modulus, and a high loss factor.

References

[1]Sun, C. T., and Chattopadhyay, S., "Dynamic Response of Anisotropic Laminated Plates Under Initial Stress Due to Impact of a Mass," *Journal of Applied Mechanics*, Vol. 43, Sept. 1975, pp. 693–698.

[2]Dobyns, A. L., "Analysis of Simply Supported Orthotropic Plates Subject to Static and Dynamic Loads," *AIAA Journal*, Vol. 19, No. 5, 1981, pp. 642–650.

[3]Whitney, J. M., and Pagano, N. J., "Shear Deformation in Heterogeneous Anisotropic Plates," *Journal of Applied Mechanics*, Vol. 37, Dec. 1970, pp. 1031–1026.

[4]Ramkumar, R. L., and Thakar, Y. R., "Dynamic Response of Curved Laminated Plates Subjected to Low Velocity Impact," *Journal of Engineering Materials and Technology*, Vol. 109, Jan. 1987, pp. 67–71.

[5]Christoforou, A. P., and Swanson, S. R., "Analysis of Simply-Supported Orthotropic Cylindrical Shells Subject to Lateral Impact Loads," *Journal of Applied Mechanics*, Vol. 57, June 1990, pp. 376–382.

[6]Gong, S. W., Toh, S. L., and Shim, V. P. W., "The Elastic Response of Orthotropic Laminated Cylindrical Shells to Low Velocity Impact," *Composites Engineering*, Vol. 4, No. 2, 1994, pp. 247–266.

[7]Gong, S. W., Shim, V. P. W., and Toh, S. L., "Impact Response of Laminated Shells with Orthogonal Curvatures," *Composites Engineering*, Vol. 5, No. 3, 1995, pp. 257–275.

[8]Gong, S. W., Shim, V. P. W., and Toh, S. L., "Central and Noncentral Normal Impact on Orthotropic Composite Cylindrical Shells," *AIAA Journal*, Vol. 34, No. 8, 1996, pp. 1619–1626.

[9]Shim, V. P. W., Toh, S. L., and Gong, S. W., "The Elastic Impact Response of Glass/Epoxy Laminated Ogival Shells," *International Journal of Impact Engineering*, Vol. 18, No. 6, 1996, pp. 633–655.

[10]Lu, C., and Lam, K. Y., "Dynamic Response of Fully-Clamped Laminated Composite Plates Subjected to Low Velocity Impact of a Mass," *International Journal of Solids and Structures*, Vol. 35, No. 11, 1998, pp. 963–979.

[11]Gong, S. W., Lam, K. Y., and Reddy, N. J., "The Elastic Response of Functionally Graded Cylindrical Shells to Low Velocity Impact," *International Journal of Impact Engineering*. Vol. 22, No. 4, 1999, pp. 397–417.

[12]Hallquist, J. O., "LS-DYNA3D—Nonlinear Dynamic Analysis of Solids in Three Dimensions," LS-DYNA3D User's Manual, Livermore Software Technology Corp., Livermore, CA, 1994.

[13]Oberst, H., "Ueber die Dampfung der Biegeschwingungen dunner Bleche durch fest haftende Blage. Akustische Beihefte," *Acustica*, Vol. 2. No. 4, 1952.

[14]Sun, C. T., and Chen, J. K., "On the Impact of Initially Stressed Composite Laminates," *Journal of Composite Materials*, Vol. 19, Nov. 1985, pp. 490–504.

[15]Wu, H. Y., "Impact Damage of Composites," Ph.D. Dissertation, Dept. of Aeronautics and Astronautics, Stanford Univ., Stanford, CA, 1986.

[16]Cairns, D. S., and Lagace, P. A., "Transient Response of Graphite/Epoxy and Kevlar/Epoxy Laminates Subjected to Impact," *AIAA Journal*, Vol. 27, No. 11, 1989, pp. 1590–1596.

A. N. Palazotto
Associate Editor